ISIJ International, Vol. 55 (2015), No. 4, pp. 736–741

Reduction and Nitriding Behavior of Hematite with Ammonia

Naoto YASUDA, Yuuki MOCHIZUKI, Naoto TSUBOUCHI and Tomohiro AKIYAMA*

Center for Advanced Research of Energy & Materials, Faculty of Engineering, Hokkaido University, Kita 13 Nishi 8, Kita-ku, Sapporo, Hokkaido, 060-8628 Japan.

(*Received on June 11, 2014; accepted on December 19, 2014*)

This paper describes the reduction and nitriding behavior of hematite with ammonia in the context of ironmaking. The effects of temperature and ammonia concentration on the products were investigated. In the temperature range from 793 to 863 K, hematite was directly reduced to magnetite by ammonia ($1/2Fe_2O_3 + 1/9NH_3 \rightarrow 1/3Fe_3O_4 + 1/6H_2O + 1/18N_2$). The ammonia started to decompose at 873 K, triggered by the generation of α-Fe. Magnetite was reduced mainly to iron by hydrogen generated from the decomposition of ammonia ($1/3Fe_3O_4 + 4/3H_2 \rightarrow Fe + 4/3H_2O$). According to in-situ X-ray diffraction (XRD) measurements, α-Fe was immediately nitrided to an ε-$Fe_{3-x}N$ ($0 \leq x \leq 1$) phase, and the N/Fe atomic ratio decreased gradually with increasing temperatures. The rate of hematite reduction increased with the ammonia concentration for 5% to 20% NH_3, but plateaus for NH_3 concentrations greater than 20%. This was attributed to the mechanism of ammonia decomposition; the amount of hydrogen generated also plateaus at ammonia concentrations above 20%. The reduction rate was therefore limited by the rate at which hydrogen was generated during ammonia decomposition. The N content of the product was affected not only by the temperature but also by the nitriding potential ($K_N = P_{NH_3}/P_{H_2}^{3/2}$). The nitriding potential increased with increasing ammonia concentrations and decreasing temperatures. The addition of nitrogen gas to the reactive gas inhibited ammonia decomposition and increased the nitrogen potential and N content of the product.

KEY WORDS: ammonia; ironmaking; hydrogen reduction; iron nitride.

1. Introduction

Although advanced energy-saving technologies are already available, the reduction of CO_2 emissions is still a subject of interest in the ironmaking industry. Ironmaking blast furnaces need approximately 500 kg of carbon source as fuel, packing material, and reducing agent to produce one ton of hot iron. In Japan, the "CO_2 Ultimate Reduction in Steelmaking process by Innovative technology for cool Earth 50 (CURSE50)" project has been in progress since 2008 with the objective of reducing CO_2 emissions from blast furnaces by approximately 30%.[1] Two approaches are possible: the CO_2 emissions from blast furnaces can either be reduced directly, or captured, separated, and recovered. For the former, the introduction into the blast furnace of hydrogen, a carbon-free reducing agent, has been discussed. Hydrogen is also expected to improve the reduction rate of iron ore. Typically however, the hydrogen is sourced from coke oven gas (COG) and is therefore not green.

Replacing carbon with hydrogen produced from non-fossil fuels would be a more effective way of reducing CO_2 emissions in the ironmaking process. This implies transporting green hydrogen from outside the ironworks, which is problematic due to the low volume energy density of hydrogen gas. Hydrogen transportation is therefore crucial for the utilization of hydrogen in the ironmaking industry. Several methods for hydrogen storage and transportation have been proposed, notably by compression, liquefaction, physisorption, and the use of metal and complex hydrides.[2]

Ammonia, which has a high hydrogen content, has attracted considerable interest in recent years as a potential hydrogen transport medium.[3–6] The storage density of ammonia is 17.6 mass% or 120 kg/m^3 for liquid NH_3, considerably higher than for most advanced metal hydrides. Ammonia gas is relatively easy to liquefy (240 K at 101 kPa) compared with hydrogen gas (140 K at 101 kPa). Furthermore, well-established production, storage, and transportation technologies are already in place since more than 160 million tons of ammonia are produced every year.[7] Ammonia is primary produced from natural gas or coal using the Haber–Bosch process, in which nitrogen reacts with hydrogen over an iron oxide catalyst.[8] Recently, Kitano *et al*. reported a novel synthesis route for ammonia using a stable electride catalyst.[9] Solid-state electrochemical synthesis is also a promising for the synthesis of ammonia from various hydrogen sources such as H_2, H_2O, CH_4, and C_2H_6.[10]

Catalytic ammonia decomposition is a key step in the utilization of ammonia as a source of hydrogen. Many catalysts have been proposed, such as Ru, Ni, Ir, Pt, Fe *etc*.[11–15] Tsubouchi *et al*. have reported the catalytic performance of fine iron particles derived from limonite ore for the removal of ammonia from fuel gas.[16,17] The results demonstrate the

* Corresponding author: E-mail: takiyama@eng.hokudai.ac.jp
DOI: http://dx.doi.org/10.2355/isijinternational.55.736

potential of iron ores as catalysts for ammonia decomposition. For the ironmaking industry, ammonia is therefore beneficial indirectly, as a source of hydrogen, but also directly, as a reducing agent, since iron ore has been shown to catalyze ammonia decomposition.

In a previous study, we reported the reduction of hematite with ammonia under 5% NH_3/Ar gas flow.[18] The reduction of hematite began at less than 773 K and was completed at 873 K, temperatures that are much lower than the 1 173 K used in conventional coal-based ironmaking. The product obtained at 723 K was a mixture of metallic iron and iron nitride. The reduction and nitriding reactions of iron oxide with ammonia are thought to be affected both by temperature and gas composition. Furthermore, these two reactions should be evaluated in comparison with hydrogen reduction. The purpose of this study was therefore to investigate the effect of ammonia concentration on the reduction and nitriding of hematite, in order to compare the reduction rate of ammonia with that of hydrogen and to understand the mechanism of ammonia reduction.

2. Experimental

The experimental apparatus is described in detail elsewhere[18] but the main features are as follows. The apparatus consists of mass flow controllers, a tubular fixed-bed reactor, a temperature controller, and a quadrupole mass spectrometer (QMS) for analyzing gaseous compounds at the reactor downstream. The mass flow controllers were connected to ammonia (99.9%), hydrogen (99.99999%), nitrogen (99.99%), and argon (99.99%). The fixed-bed reactor was a transparent quartz tube with an inner diameter of 6 mm. The fixed bed was 270 mg of hematite powder (α-Fe_2O_3, 99.9% purity grade, Kojundo Chemical Laboratory Co., Ltd.) with a particle diameter of ca. 1 μm. This was supported by quartz wool. The fixed-bed temperature was monitored and controlled using a K-type thermocouple placed underneath the quartz wool.

Table 1 lists the experimental conditions used for the ammonia (or hydrogen) reduction of hematite. The mixed reducing gases, whose compositions are shown in Table 1, were first flowed to replace the atmosphere in the fixed bed. Having confirmed this replacement by QMS, the fixed bed was heated at a rate of 10 K·min^{-1} up to the designated holding temperature, which was maintained for at least 2 h to complete the reduction reaction. The gas was then replaced by pure argon at a rate of 200 cm^3·min^{-1} at standard temperature and pressure (STP). Finally, the fixed bed was cooled down to ambient temperature.

Table 1. Experimental conditions for the reduction of hematite powder.

Run No.	Concentration of reducing gas [mol%]	Flow rate [cm^3 min^{-1}(STP)]				Holding Temperature [K]
		NH_3	H_2	N_2	Ar	
A10-500	10.0	20	0	0	180	773
A10-600	10.0	20	0	0	180	873
A10-700	10.0	20	0	0	180	973
A05-700	5.0	10	0	0	190	973
A20-700	20.0	40	0	0	160	973
A30-700	30.0	60	0	0	140	973
H07-700	7.1	0	15	0	195	973
H14-700	13.6	0	30	0	190	973
H25-700	25.0	0	60	0	180	973
H35-700	34.6	0	90	0	170	973
A20N20-700	20.0	40	0	40	120	973
A20N40-700	20.0	40	0	80	80	973

The flow rate of NH_3 in the exhaust gas can be determined from the intensity of the NH_3 and Ar QMS peaks.

$$I_{NH_3} \propto C_{NH_3} = \frac{F_{NH_3}}{\sum F_i} \quad \text{..... (1)}$$

$$I_{Ar} \propto C_{Ar} = \frac{F_{Ar}}{\sum F_i} \quad \text{..... (2)}$$

$$\frac{I_{NH_3}}{I_{Ar}} \propto \frac{F_{NH_3}}{F_{Ar}} \quad \text{..... (3)}$$

$$F_{NH_3} = a_1 F_{Ar} \frac{I_{NH_3}}{I_{Ar}} + b_1 \quad \text{..... (4)}$$

where I, C, and F denote the QMS intensity and the concentration and flow rate in the exhaust gas, respectively. The QMS intensities, I^f, of the NH_3 fragments, N_2 and H_2, can be used to calculate the flow rates as follows:

$$F_{N_2} = a_2 F_{Ar} \frac{\left(I_{N_2} - I^f_{N_2}\right)}{I_{Ar}} + b_2 \quad \text{..... (5)}$$

$$I^f_{N_2} = c_2 I_{NH_3} + d_2 \quad \text{..... (6)}$$

$$F_{H_2} = a_3 F_{Ar} \frac{\left(I_{H_2} - I^f_{H_2}\right)}{I_{Ar}} + b_3 \quad \text{..... (7)}$$

$$I^f_{H_2} = c_3 I_{NH_3} + d_3 \quad \text{..... (8)}$$

According to a preliminary experiment, the standard errors were estimated to be less than ± 3 cm^3·min^{-1} for NH_3, H_2, and, N_2 flow rates ranging from 0 to 40 cm^3·min^{-1}. The error increased to ± 3 cm^3·min^{-1} for flow rates greater than 40 cm^3·min^{-1}. Reduction in this temperature range is characterized by the generation of steam. In fact, no NO_x gas was detected at any temperature. The reduction rate was estimated from the integrated intensity of the H_2O peak, $I^f_{H_2O}$, normalized to that of Ar. The overlap between the H_2O and NH_3 peaks in the QMS spectra should also be considered because the mass numbers of the two compounds are close.

$$I'_{H_2O} = \frac{I_{H_2O} - I^f_{H_2O}}{I_{Ar}} \quad \text{..... (9)}$$

$$I^f_{H_2O} = c_4 I_{NH_3} + d_4 \quad \text{..... (10)}$$

All coefficients (a, b, c, and d) were determined using calibration curves.

After these experiments, the crystalline phases in the solid products were identified by X-ray diffraction (XRD, Miniflex, Rigaku Co., Ltd.). The nitrogen content in the samples was measured by elemental analysis (MT-6 CHN

Corder, Yanaco Technical Science Co., Ltd.). In-situ XRD analysis was performed in order to examine the reduction and nitriding behaviors with ammonia. The analytical conditions have been reported in detail elsewhere.[19] XRD patterns were first recorded at 298 K under flowing 5% NH_3 balanced by helium. Each specimen was then heated at 10 $K \cdot min^{-1}$ up to a predetermined temperature, which was held for 30 min prior to further measurements.

3. Results and Discussion

3.1. Mechanisms of Hematite Reduction and Nitriding with Ammonia

Figure 1 shows the changes in the flow rate of ammonia with time in the exhaust gas during heating up and holding at 773, 873, and 973 K. For A10-600 and A10-700, the flow rate of ammonia started to decrease at approximately 873 K. The decrease of ammonia was attributed to reduction and/or to ammonia decomposition. At 9.0 ks, the ammonia decomposition percentages for A10-500, A10-600, and A10-700 were 5, 53, and 82%, respectively. Ammonia was therefore scarcely decomposed at 773 K. **Figure 2** shows the XRD profiles of the samples in the fixed-bed reactor after the reduction. Hematite reduced to magnetite at 773 K and to iron or iron nitrides at temperatures greater than 873 K. These results indicate that ammonia decomposition was triggered by the formation of metallic iron. The products were mixtures of γ'-Fe_4N and ε-$Fe_{3-x}N$ ($0 \le x \le 1$) phases at 873 K and α-Fe and γ'-Fe_4N phases at 973 K, indicating that the iron nitrides decomposed at higher temperatures.

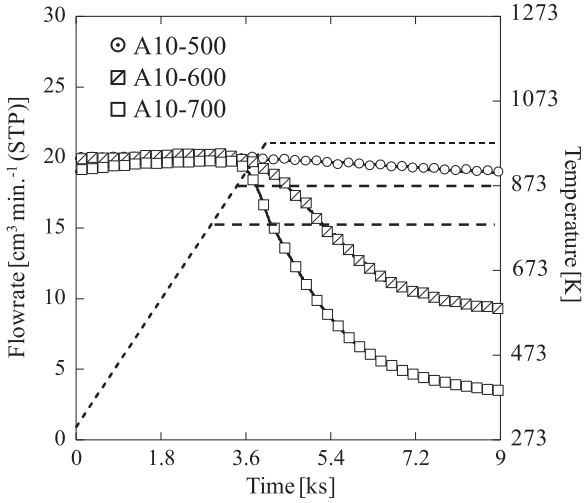

Fig. 1. Changes in the flow rate of ammonia in exhaust gas during heating up and holding at 773, 873, and 973 K.

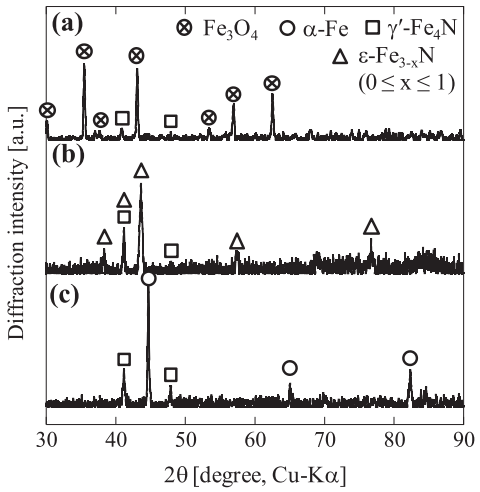

Fig. 2. XRD profiles of the samples reduced at different temperatures: (a) A10-500, (b) A10-600, and (c) A10-700.

Figure 3 shows changes in the differential of relative intensity for each gas component during heating to 973 K under flowing 10% NH_3 (A10-700). The values were normalized to the maximum differential intensity. Nitrogen and steam were generated at temperatures of ~793 K and above. Steam is the gas component that contains O atoms and therefore evidences the reduction of hematite. The differential intensity for steam shows an initial peak at 863 K, which was attributed to the reduction of hematite to magnetite. No hydrogen gas was detected from 793 to 863 K, indicating either that the hematite was directly reduced by ammonia, or that the hydrogen generated by the decomposition of ammonia was immediately consumed by the reduction. In either case, the overall reaction for temperatures between 793 and 863 K can be expressed as follows:

$$1/2Fe_2O_3 + 1/9NH_3 \rightarrow 1/3Fe_3O_4 + 1/6H_2O + 1/18N_2 \quad .....(11)$$

In contrast, the differential intensit for all gas components increased rapidly from 873 to 973 K. This result can be explained by the reduction and decomposition of ammonia. Ammonia decomposition was triggered by the formation of metallic iron, as mentioned above. In other words, the reduced iron served as a catalyst for ammonia decomposition. The mechanism and kinetics of ammonia decomposition over iron catalysts have been well studied.[20–23] Following the generation of hydrogen due to the ammonia decomposition at approximately 873 K, the differential intensity for steam increased again. Moreover, the reduction rate of ammonia was slower than that of hydrogen, as discussed in detail below. Therefore, we concluded that magnetite was mainly reduced to iron by the hydrogen generated through the decomposition of ammonia.

$$1/3Fe_3O_4 + 4/3H_2 \rightarrow Fe + 4/3H_2O \quad ..... (12)$$

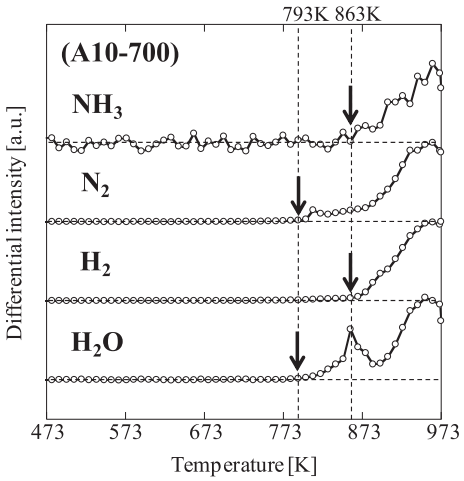

Fig. 3. Changes in the differential of relative intensity for each gas component during heating up to 973 K. The values were normalized to the maximum differential intensity.

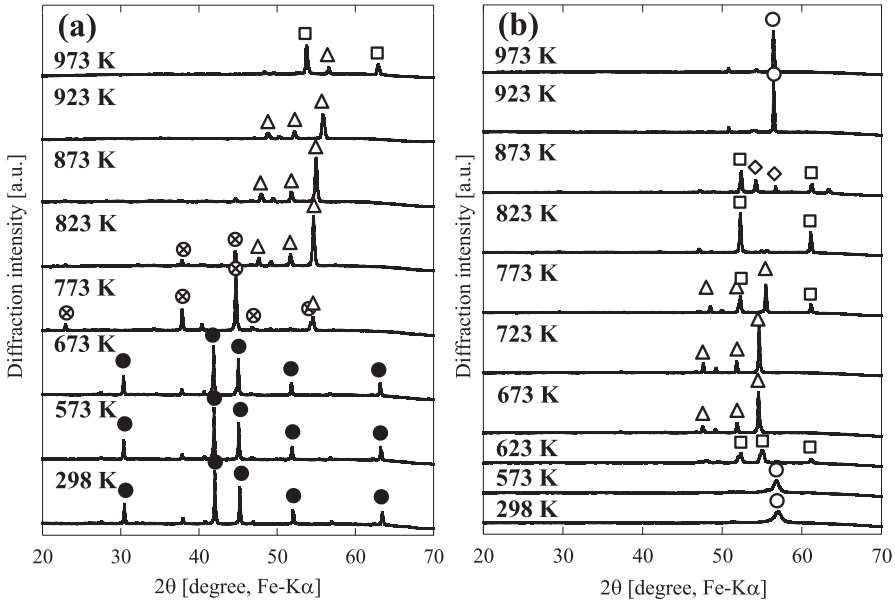

Fig. 4. In-situ XRD profiles during heating of (a) hematite and (b) metallic iron in a stream of 5% NH_3 diluted with helium: (○) α-Fe; (□) γ'-Fe_4N; (△) ε-$Fe_{3-x}N$ ($0 \le x \le 1$); (◇) α''-$Fe_{16}N_2$; (⊗) Fe_3O_4; (●) Fe_2O_3.

According to the XRD patterns, the reduced iron was nitrided by ammonia, and the nitride then decomposed at higher temperatures.

$$y\mathrm{Fe} + \mathrm{NH_3} \rightarrow \mathrm{Fe}_y\mathrm{N} + 3/2\mathrm{H_2} \quad \text{..... (13)}$$

$$\mathrm{Fe}_y\mathrm{N} \rightarrow y\mathrm{Fe} + 1/2\mathrm{N_2} \quad \text{..... (14)}$$

Nitriding is a reaction between iron and atomic nitrogen generated by the dissociative adsorption of ammonia molecules on the iron surface.

$$\mathrm{NH_3} \rightarrow [\mathrm{N}]_{\mathrm{ad}} + 3/2\mathrm{H_2} \quad \text{..... (15)}$$

In contrast, nitrogen molecules do not contribute to the nitriding reaction because of the extremely large N≡N bond energy (945 kJ·mol^{-1}).[24]

In order to confirm the dynamic behavior of the reduction and nitriding of hematite with ammonia, commercial hematite and metallic iron reagents were subjected to in-situ XRD measurements. **Figure 4** shows the in-situ XRD profiles obtained during heating from 298 to 973 K of the two reagents in a stream of 5% NH_3 diluted with helium. In a preliminary experiment, an alumina reagent was added to correct the angular error due to the volume expansion of the sample. The peaks of the alumina reagent shifted to smaller angles by 0.2–0.4°, with this difference increasing with the diffraction angle. The product phases were therefore indexed in consideration of this error. Although the experimental conditions for the in-situ XRD analysis differed slightly from those in the fixed-bed reactor, the same tendencies were observed as those described above. The hematite reduced to magnetite at 773 K and the latter was directly nitrided to ε-$Fe_{3-x}N$ at 823 K. This result indicates that the reduction-generated α-Fe was immediately nitrided at this temperature. The ε-$Fe_{3-x}N$ phase gradually decomposed to γ'-Fe_4N and α-Fe with increasing temperature because iron nitride decomposition (Eq. (14)) dominated at high temperatures. In contrast, the nitriding of the iron reagent began at 623 K. This therefore confirmed that under these conditions, hematite was nitrided via the generation of α-Fe. The nitriding reaction dominated up to a temperature of 723 K, above which the iron nitride gradually decomposed. This nitriding behavior agrees with the results obtained by Arabczyk *et al*.[25]

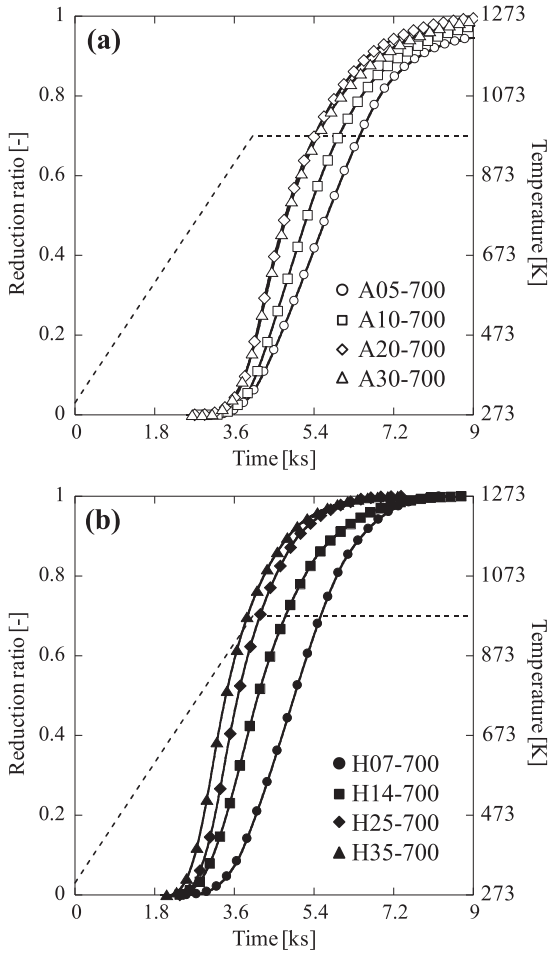

Fig. 5. Changes in the reduction ratio at different concentrations of (a) ammonia and (b) hydrogen flows, as estimated from the QMS intensity of H_2O in the exhaust gas.

3.2. The Effect of Ammonia Concentration on the Reduction and Nitriding of Hematite

Figure 5 shows the changes in the reduction ratio under ammonia and hydrogen flows, as estimated from the QMS intensity of steam in the exhaust gas. The reduction experiments were performed at 5, 10, 20, and 30% NH_3, and at 7, 14, 25, and 35% H_2, as shown in Table 1. Each hydrogen concentration corresponds to the concentration that is reached when the ammonia is completely decomposed to nitrogen and hydrogen. The reduction rate of hematite increased with the ammonia concentration from 5% to 20% NH_3, but plateaus thereafter. In contrast, no saturation is observed in the reduction rate, even at 35% H_2. Ammonia reduction proceeded more slowly than hydrogen reduction.

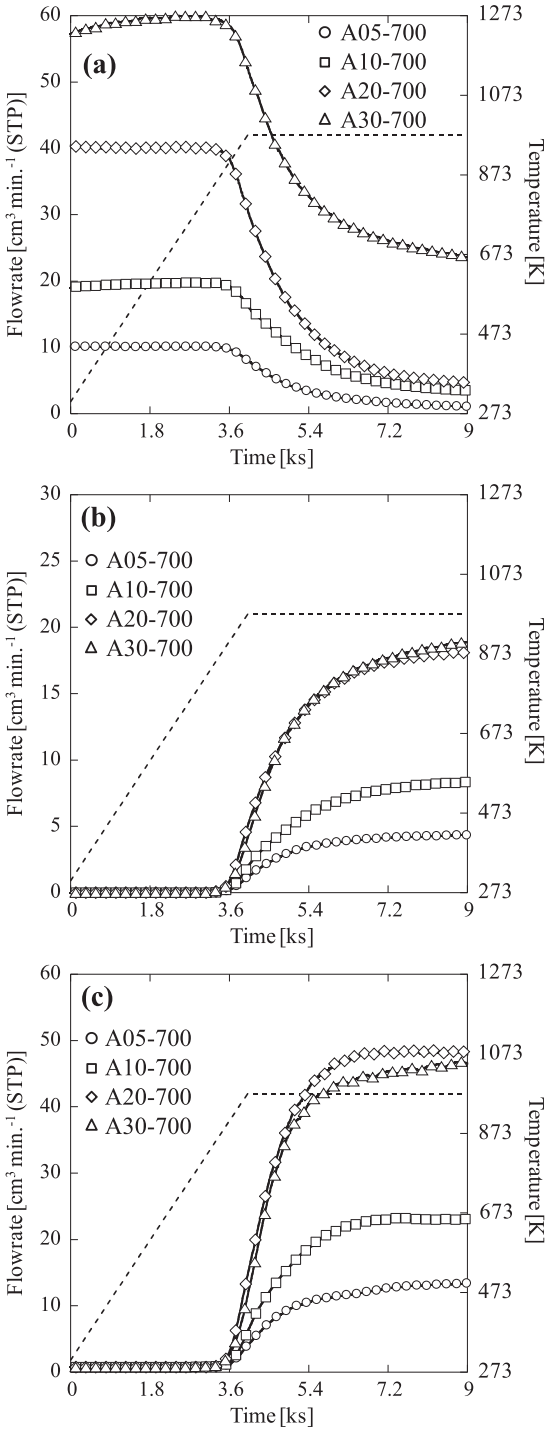

Fig. 6. Changes in the flow rate of (a) ammonia, (b) nitrogen, and (c) hydrogen at different ammonia inflow during heating up to 973 K and then holding at this temperature.

Figure 6 shows the changes in the flow rate of ammonia, nitrogen, and hydrogen in the exhaust gas during heating up to 973 K and then holding at this temperature. Ammonia decomposition started at approximately 873 K, regardless of the ammonia concentration. However, **Table 2** shows that the decomposition rate of A30-700 was significantly lower than for the other runs. After 873 K, the flow rate of nitrogen and hydrogen generated due to ammonia decomposition increased with the ammonia concentration from 5% to 20% NH_3, but plateaus thereafter, following the same trend as the reduction rate. This result supports the idea that magnetite was reduced mainly to iron by the generated hydrogen. The reduction rate was limited by the hydrogen flow at temperatures above 873 K.

Figure 7 shows the XRD profiles of the samples in the fixed-bed reactor after the reduction of hematite under 5, 10, 20, and 30% NH_3 flows. The nitriding of the products was clearly in proportion to the ammonia concentration. Note that as mentioned above, nitriding is a reaction between iron and atomic nitrogen generated on the iron surface. Nitriding should be promoted as the amount of decomposed ammonia

Table 2. Relationship between the reaction behavior of ammonia decomposition and the nitrogen content of samples after the experiments.

Sample	Flow rate of NH_3 [cm^3 min^{-1} (STP)]		Decomposition rate of NH_3 [%]	Nitriding potential* (K_N) [–]	Nitrogen content of sample [%]
	Inflow	Outflow at 9.0 ks			
A10-500	20	19.0	5	79	3.7
A10-600	20	9.3	53	1.9	8.1
A10-700	19	3.5	82	0.42	2.9
A05-700	10	1.1	89	0.30	0.6
A20-700	40	4.6	88	0.18	3.3
A30-700	57	24	59	0.90	7.6
A20N20-700	38	8.5	78	0.39	4.2
A20N40-700	42	10	75	0.47	5.5

* $K_N = P_{NH_3}/P_{H_2}^{3/2}$

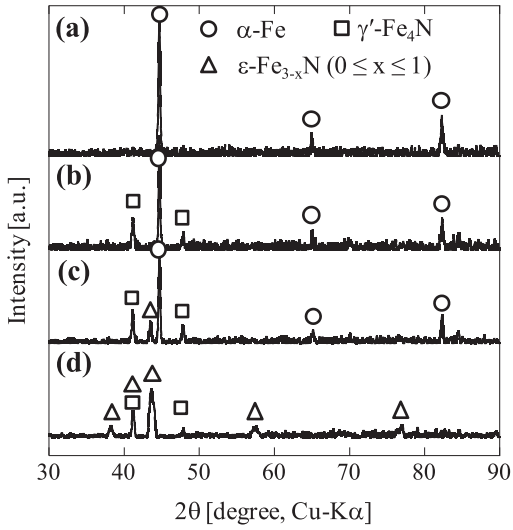

Fig. 7. XRD patterns of the samples reduced at different ammonia concentrations: (a) A05-700, (b) A10-700, (c) A20-700, and (d) A30-700.

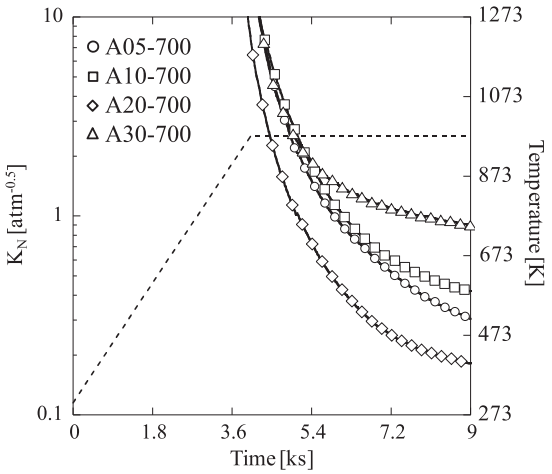

Fig. 8. Changes in the nitriding potential at different ammonia inflows, which were calculated from the following equation: $K_N = P_{NH_3}/P_{H_2}^{3/2}$.

on the iron surface is increased. However, the N content of the A30-700 sample was significantly higher than that of the other products, in spite of ammonia decomposition rates on its surface being similar to those for A20-700. This result can be explained by differences in the nitriding potential, K_N, which is defined as the inverse of the equilibrium constant of the nitriding reaction (Eq. (15)).

$$K_N = P_{NH_3} / P_{H_2}^{3/2} \quad \text{..... (16)}$$

Figure 8 shows the changes in K_N for these samples during heating to 973 K and then holding. It should be noted that the value of K_N under 30% NH_3 flow was four times higher than under 20% NH_3 flow since the ammonia decomposition rate was quite low, as shown in Fig. 6 and Table 2. In order to confirm the effect of K_N on the nitriding of the samples, the argon in the reactive gas was partially substituted by nitrogen (A20N20-700 and A20N40-700 in Table 1). Table 2 summarizes the relationship between the reaction behavior of the ammonia decomposition and the nitrogen content of the samples after the experiments. The addition of nitrogen inhibited ammonia decomposition owing to equilibrium shift. As a result, K_N and the N content of the product increased with the nitrogen concentration. Therefore, it was concluded that the N content of the product was affected by the temperature, the ammonia concentration, and the nitriding potential of the reaction environment.

4. Conclusions

The reduction and nitriding behavior of hematite with ammonia were compared, leading to the following conclusions:

(1) The reduction and nitriding of hematite with ammonia can be described as follows:

(i) Hematite was directly reduced to magnetite by ammonia for temperatures ranging from 793 to 863 K ($1/2Fe_2O_3 + 1/9NH_3 \rightarrow 1/3Fe_3O_4 + 1/6H_2O + 1/18N_2$).

(ii) Ammonia decomposition began at 873 K, which was triggered by the generation of α-Fe. After the generation of hydrogen due to the ammonia decomposition, the magnetite phase was reduced mainly to α-Fe by hydrogen ($1/3Fe_3O_4 + 4/3H_2 \rightarrow Fe + 4/3H_2O$).

(iii) The α-Fe formed by reduction was immediately nitrided to an ε-$Fe_{3-x}N$ phase, which then gradually decomposed to γ'-Fe_4N and α-Fe at higher temperatures at which the driving force for decomposition became stronger than for iron nitride formation.

(2) The hematite reduction rate and the hydrogen flow rate generated by ammonia decomposition both increased as the ammonia concentration was increased from 5% to 20%, but plateau thereafter. This indicates that under these conditions, the reduction rate was limited by the hydrogen flow rate.

(3) The N content of the product was affected by the temperature, ammonia concentration, and nitriding potential, K_N, of the reaction environment. The addition of nitrogen in the reactive gas inhibited the decomposition of ammonia owing to equilibrium shift. As a result, K_N and the N content of the product increased with the nitrogen concentration.

These results should prove valuable to promote the utilization of ammonia as a reducing agent in the ironmaking industry.

Acknowledgments

This research was supported by a Grant-in-Aid for JSPS Fellows (23·3412).

REFERENCES

1) S. Tonomura: *Energy Procedia*, **37** (2013), 7160.
2) L. Zhou: *Renew. Sust. Energ. Rev.*, **9** (2005), 395.
3) A. Klerke, C. H. Christensen, J. K. Norskov and T. Vegge: *J. Mater. Chem.*, **18** (2008), 2304.
4) C. Zamfirescu and I. Dincer: *Fuel Process. Technol.*, **90** (2009), 729.
5) R. Lan, J. T. S. Irvine and S. Tao: *Int. J. Hydrogen Energ.*, **37** (2012), 1482.
6) F. Schuth, R. Palkovits, R. Schlogl and D. S. Su: *Energy Environ. Sci.*, **5** (2012), 6278.
7) International Fertilizer Industry Association: World NH3 Statistics by Country, http://www.fertilizer.org/ifa/HomePage/STATISTICS/Production-and-trade, (accessed 2013-11-17).
8) M. Appl: The Haber–Bosch Heritage: The Ammonia Production Technology. 50th Anniversary of the IFA Technical Conf., International Fertilizer Industry Association, Paris, (1997), 1.
9) M. Kitano, Y. Inoue, Y. Yamazaki, F. Hayashi, S. Kanbara, S. Matsuishi, T. Yokoyama, S.-W. Kim, M. Hara and H. Hosono: *Nat. Chem.*, **4** (2012), 934.
10) I. Amar, R. Lan, C. G. Petit and S. Tao: *J. Solid State Electrochem.*, **15** (2011), 1845.
11) T. V. Choudhary, C. Sivadinarayana and D. W. Goodman: *Catal. Lett.*, **72** (2001), 197.
12) A. S. Chellappa, C. M. Fischer and W. J. Thomson: *Appl. Catal. A*, **227** (2002), 231.
13) S. F. Yin, B. Q. Xu, X. P. Zhou and C. T. Au: *Appl. Catal. A*, **277** (2004), 1.
14) F. R. García-García, Y. H. Ma, I. Rodríguez-Ramos and A. Guerrero-Ruiz: *Catal. Commun.*, **9** (2008), 482.
15) J. Donald, C. Xu, H. Hashimoto, E. Byambajav and Y. Ohtsuka: *Appl. Catal. A*, **375** (2010), 124.
16) N. Tsubouchi, H. Hashimoto and Y. Ohtsuka: *Catal. Lett.*, **105** (2005), 203.
17) N. Tsubouchi, H. Hashimoto and Y. Ohtsuka: *Energ. Fuel.*, **21** (2007), 3063.
18) S. Hosokai, Y. Kasiwaya, K. Matsui, N. Okinaka and T. Akiyama: *Environ. Sci. Technol.*, **45** (2010), 821.
19) Y. Ohshima, N. Tsubouchi and Y. Ohtsuka: *Appl. Catal. B-Environ.*, **111–112** (2012), 614.
20) S. Brunauer, K. S. Love and R. G. Keenan: *J. Am. Chem. Soc.*, **64** (1942), 751.
21) D. G. Löffler and L. D. Schmidt: *J. Catal.*, **44** (1976), 244.
22) G. Ertl and M. Huber: *J. Catal.*, **61** (1980), 537.
23) W. Arabczyk and J. Zamlynny: *Catal. Lett.*, **60** (1999), 167.
24) S. Gambarotta and J. Scott: *Angew. Chem. Int. Ed.*, **43** (2004), 5298.
25) W. Arabczyk, J. Zamłynny and D. Moszyński: *Pol. J. Chem. Technol.*, **12** (2010), 38.